

# A NOVEL ML BASED JOINT TOA AND AOA ESTIMATOR FOR IR-UWB SYSTEMS

*Fang Shang, Benoit Champagne and Ioannis Psaromiligkos*

Department of Electrical and Computer Engineering, McGill University  
3480 University Street, Montreal, Quebec, Canada, H3A 2A7

{fang.shang@mail.mcgill.ca; benoit.champagne@mcgill.ca; ioannis.psaromiligkos@mcgill.ca}

## ABSTRACT

A novel joint TOA and AOA estimator is proposed for impulse radio Ultra-Wideband (IR-UWB) systems, in which a uniform linear array of antennas is employed at the receiver. The proposed method consists of two steps: (1) coarse estimation of the TOA and the average power delay profile; (2) joint TOA refinement and AOA estimation by maximization of a novel log likelihood function (LLF) using the coarse estimates from the first step. The derivation of the LLF is based on an original approach in which the pulse image from the primary path is modeled as a deterministic component while the superposition of the images from the secondary paths is modeled as a Gaussian random process. In addition, a special gating mechanism is used to characterize the secondary paths, thereby leading to a previously unknown form of the LLF in step (2). According to simulation experiments based on standard UWB channel models, our approach exhibits superior performance to that of a competing scheme from the recent literature.

**Index Terms**— Ultra wideband, angle of arrival, time of arrival, average power delay profile, maximum likelihood

## 1. INTRODUCTION AND RELATION TO PRIOR WORK

Due to the fine time resolution nature of ultra wideband (UWB) signals, time of arrival (TOA) estimation with very high accuracy can be achieved in UWB systems. As a consequence, indoor localization of objects using impulse radio UWB (IR-UWB) technology has been gaining wide acceptance [1]. In a line of sight (LOS) radio environment, assuming a planar geometry, estimation of the TOA of the transmitted pulses by three or more (non-collinear) receivers enables the localization of the desired source through multilateration [2]. The number of required receivers for localization can be reduced and the performance of positioning systems can be further improved if the angles-of-arrival (AOA) of the transmitted pulses can also be estimated. To this end, the receiver must be equipped with an array of antennas and have the capability to process their outputs coherently, allowing for the extraction of spatial information.

Initial attempts in AOA estimation for UWB signals focused on subspace methods [3, 4]. To apply the traditional subspace method (as in the narrowband case) to UWB signals, a focusing technique must be employed [3]. However, subspace-based methods have very high complexity (as they require an eigenvalue decomposition) and lead to large estimation errors in rich multipath environments. Recently, there has been much interest in the investigation of new AOA estimation approaches based on time difference of arrival (TDOA). TDOA-based methods normally estimate the TOA and AOA using

a receiver equipped with an antenna array, such as a uniform linear array (ULA) or a uniform circular array (UCA). In [5], for example, joint estimation is performed by calculating a two dimensional power delay-angle spectrum within the frequency domain. In [6], a frequency domain approach is also adopted for the joint estimation of TOA and AOA. In [7], a joint TOA/AOA estimator is proposed for UWB indoor ranging under line-of-sight (LOS) operating conditions, in which signal samples obtained from an antenna array at the Nyquist rate are processed in a three-step algorithm to produce TOA and AOA estimates. These recent methods first obtain TOA estimates at each antenna (either via time- or frequency-domain processing), and then extract the desired AOA by computing TDOAs. Although their performance is competitive to early schemes [3, 4], the imposed processing structure limits the achievable accuracy of the AOA estimate and suggests that other estimators with better performance may exist.

In this paper, we present a novel joint estimator of TOA and AOA for a multi-antenna IR-UWB receiver based on the maximum likelihood (ML) criterion. The proposed estimator is obtained in two steps: (1) coarse estimation of the TOA and the average power delay profile (APDP); (2) joint refinement of the TOA and estimation of the AOA by maximization of a novel log likelihood function (LLF) using the coarse estimates from the first step. Besides the coarse TOA estimation, the first step includes the estimation of the APDP using least-squares (LS) fitting to a decaying exponential model, which is not found in prior methods. One of the key features of our proposed approach lies in the choice of a novel statistical model, in which the primary and secondary pulse images are represented by a deterministic component and a zero-mean Gaussian random process, respectively. In particular, this model employs time-shifted gating functions to characterize the onset of the secondary paths, which in turn leads to a previously unknown form of the LLF in step (2). Through numerical simulations based on standard UWB channel models, the proposed 2-step approach for joint TOA and AOA estimation is shown to outperform a competing benchmark method [7] from the literature.

The rest of this paper is organized as follows. Section 2 gives a description of the system model. Section 3 presents the derivation of the underlying log likelihood function. Section 4 presents the proposed algorithm. Simulation results are discussed in Section 5 and Section 6 concludes the paper.

## 2. SYSTEM MODEL

According to the IEEE 802.15.4a standard, TOA estimation is performed during the ranging preamble of a synchronization header [8]. The transmitted signal  $s(t)$  consists of  $N_s$  consecutive symbols of duration  $T_b$ , spanning a total interval (observation time) of

This work was supported in part by the Fonds Québécois de la Recherche sur la Nature et les Technologies.

$T_o = N_s T_b$ , and can be expressed as

$$s(t) = \sum_{j=0}^{N_s-1} a_j \sqrt{E_p} w(t - jT_b), \quad 0 \leq t \leq T_o \quad (1)$$

where  $w(t)$  is a pulse waveform with duration  $T_c$ ,  $E_p$  denotes the transmitted energy per pulse and  $\{a_j\}$  is a sequence of information symbols taking values from  $\{+1, -1\}$ . Without loss in generality, a ranging sequence with  $a_j = 1, \forall j$ , is adopted for ranging.

The transmitted IR-UWB signal  $s(t)$  propagates through a linear time-invariant multi-path channel before reaching the IR-UWB receiver. The latter is equipped with a ULA of  $Q \geq 2$  identical antenna elements. Under the far field assumption, the wavefronts arriving at the receiver's ULA along different paths can be taken as planar. In particular, for the primary path (the first one in a LOS environment), the TOA at the  $q$ th antenna can be written as

$$\tau_q = \tau + q\Delta\tau, \quad q \in \{0, \dots, Q-1\} \quad (2)$$

where  $\tau$  denotes the TOA at the reference antenna ( $q = 0$ ) and  $\Delta\tau$  is the TDOA between adjacent antennas. For a 2-dimensional geometry, the TDOA can be expressed in terms of the AOA,  $\theta$ , as  $\Delta\tau = \frac{d}{c} \cos \theta$ , where  $d$  is the inter-antenna spacing and  $c$  is the speed of light.

The propagation channel is modeled as a linear time-invariant single-input multiple-output (SIMO) system with components  $\mathcal{H}_q\{\cdot\}$ . We represent the channel response to the pulse waveform  $w(t)$  at the  $q$ th antenna as a superposition of two distinct components:

$$\mathcal{H}_q\{w(t)\} = \eta(t - \tau_q) + \zeta_q(t) \quad (3)$$

where  $\eta(t)$  represents the image of pulse  $w(t)$  arriving along the primary path, and  $\zeta_q(t)$  represents the total contribution of the images received along the secondary paths, i.e., excluding the primary one. We assume that the self-interference between successive symbols is negligible, that is:  $T_c + \tau_{ds} < T_b$ , where  $\tau_{ds}$  is the maximum delay spread of the channel.

We model the primary pulse image  $\eta(t)$  as a deterministic signal and the superimposed secondary pulse images  $\zeta_q(t)$  as independent Gaussian random processes with zero mean and instantaneous power (variance)

$$\sigma_q^2(t) = g(t - \tau_q - T_c)P(t) \quad (4)$$

where  $P(t)$  is the APDP (for an impulse emitted at time 0) and  $g(t)$  is a gating function used to model the onset of the secondary pulse image after the primary one at  $t = \tau_q$ . The additional delay of  $T_c$  in (4) is introduced to account for the duration of the first pulse image, assumed to be of width  $T_c$ . Although in practice the primary path is not always resolvable, this assumption is still effective in the application of our approach as checked in the simulations later. As a gating function, we adopt a unit step, i.e.,  $g(t) = 0$  for  $t < 0$  and 1 for  $t \geq 0$ , but other choices are possible. The APDP typically takes the form of multiple exponentially decaying clusters whose parameters can be estimated using the techniques in [9]. It can also be roughly represented by a single decaying exponential function.

Furthermore, we model the space-time cross correlation between the secondary pulse image signals as

$$E[\zeta_q(t)\zeta_{q'}(u)] = \sigma_q(t)\sigma_{q'}(u)\delta(t-u)\varrho(q, q') \quad (5)$$

where  $\delta(t)$  is the Dirac delta function and  $\varrho(q, q')$  is the spatial correlation. The use of  $\delta(t-u)$  is motivated by the fact that the extent of the temporal correlation for multipath components is usually very small [10, 11]. For a dense multipath environment, the spatial correlation decreases rapidly with the inter-antenna spacing [12], and

accordingly, we set  $\varrho(q, q') = 1$  for  $q = q'$  and 0 otherwise, although a more general model could be employed.

Finally, the noisy IR-UWB signal received at the  $q$ th antenna after multipath propagation, can be expressed as

$$r_q(t) = \mathcal{H}_q\{s(t)\} + n_q(t), \quad 0 \leq t \leq T_o \quad (6)$$

where  $n_q(t)$  is an additive noise term modeled as a spatially and temporally white Gaussian process with zero mean and known power spectral density level  $\sigma_n^2$ . We assume that the noise terms  $n_q(t)$  are statistically independent from the secondary pulse images  $\zeta_{q'}(t)$ .

In this work, our goal is to jointly estimate the TOA and AOA of the primary path, which is equivalent to estimating  $\tau$  and  $\Delta\tau$  in (2), from the received antenna signals  $\{r_q(t)\}$  for  $0 \leq t \leq T_o$  and  $q \in \{0, \dots, Q-1\}$ .

### 3. DERIVATION OF THE JOINT LLF

We assume that the observed antenna signals  $r_q(t)$  in (6) are uniformly sampled at the rate  $F_s$ . Specifically, we let  $t = nT_s$  where  $t$  is limited  $0 \leq t < T_o$  and  $T_s$  denotes the sampling period, which is assumed to satisfy the Nyquist criterion for bandpass signals, that is: the sampling frequency  $F_s = 1/T_s \geq 2B$ . For simplicity, we also assume that each symbol consists of exactly  $M$  time samples, i.e.,  $T_b = MT_s$  where  $M$  is a positive integer.

As in previous works [6, 7], to improve the processing gain, the received signals are first averaged over the  $N_s$  symbols comprising the observation interval. Accordingly, let us introduce

$$\mathbf{x}(t) \equiv [x_0(t), \dots, x_{Q-1}(t)]^T \quad (7)$$

$$= \frac{1}{N_s} \sum_{j=0}^{N_s-1} \mathbf{r}_j(t) = \boldsymbol{\mu}(t) + \boldsymbol{\xi}(t) + \mathbf{n}(t) \quad (8)$$

where we define

$$\mathbf{r}_j(t) = [r_0(t + jT_b), \dots, r_{Q-1}(t + jT_b)]^T \quad (9)$$

$$\boldsymbol{\mu}(t) = \sqrt{E_p}[\eta(t - \tau_0), \dots, \eta(t - \tau_{Q-1})]^T \quad (10)$$

$$\boldsymbol{\xi}(t) = \sqrt{E_p}[\zeta_0(t), \dots, \zeta_{Q-1}(t)]^T \quad (11)$$

$$\mathbf{n}_j(t) = [n_0(t + jT_b), \dots, n_{Q-1}(t + jT_b)]^T \quad (12)$$

and thus the additive noise term becomes  $\mathbf{n}(t) = \frac{1}{N_s} \sum_j \mathbf{n}_j(t)$ . In (7), discrete-time  $t = nT_s$  is now restricted to the interval  $[0, T_b)$ , or equivalently  $n \in \{0, 1, \dots, M-1\}$ .

Invoking the Gaussian assumption on the multipath signals and background noise processes, it follows that  $\mathbf{x}(t)$  is a vector Gaussian process with non-zero mean,  $E[\mathbf{x}(t)] = \boldsymbol{\mu}(t)$ , and  $Q \times Q$  matrix auto-covariance function

$$\begin{aligned} \mathbf{K}_x(t, u) &= E[(\mathbf{x}(t) - \boldsymbol{\mu}(t))(\mathbf{x}(u) - \boldsymbol{\mu}(u))^T] \\ &= \mathbf{K}_\xi(t, u) + \mathbf{K}_n(t, u) \end{aligned} \quad (13)$$

where we define  $\mathbf{K}_\xi(t, u) = E[\boldsymbol{\xi}(t)\boldsymbol{\xi}(u)^T]$  and  $\mathbf{K}_n(t, u) = E[\mathbf{n}(t)\mathbf{n}(u)^T]$ ,  $u$  being a discrete-time variable with the same range as  $t$ . Taking into account the band-limited (anti-aliasing) filtering implicit in the uniform sampling of the antenna signals, the matrix auto-covariance function of the additive noise  $\mathbf{n}(t)$  takes the form

$$\mathbf{K}_n(t, u) = \delta(t-u) \frac{\sigma_n^2}{T_s} \mathbf{I}_Q \quad (14)$$

where  $\sigma_n^2 = \sigma_n^2/N_s$ ,  $\delta(t)$  now represents the Kronecker (discrete-time) delta function ( $\delta(nT_s) = 1$  if  $n = 0$  and 0 otherwise) and  $\mathbf{I}_Q$

is an identity matrix of size  $Q$ . Similarly, but this time taking into account the definition of  $\boldsymbol{\xi}(t)$  in (11) and the statistical properties of  $\zeta_q(t)$  over the spatial dimension as per (5), we obtain

$$\mathbf{K}_\xi(t, u) = \delta(t - u) \frac{E_p}{T_s} \mathbf{D}(t) \quad (15)$$

where  $\mathbf{D}(t)$  is a  $Q \times Q$  diagonal matrix with diagonal entries  $\sigma_q^2(t)$ . Therefore, we can finally express the matrix auto-covariance function of  $\mathbf{x}(t)$  as follows,

$$\mathbf{K}_x(t, u) = \delta(t - u) \frac{1}{T_s} (E_p \mathbf{D}(t) + \sigma_n^2 \mathbf{I}_Q) \quad (16)$$

Obviously,  $\mathbf{K}_x(t, u)$  is also a diagonal matrix function.

Define the vector of parameters  $\boldsymbol{\theta} = [\tau, \Delta\tau, \boldsymbol{\theta}_\eta, \boldsymbol{\theta}_\zeta]$ , where  $\boldsymbol{\theta}_\eta$  contains the nuisance parameters associated to the pulse image from the primary path,  $\eta(t)$ , and  $\boldsymbol{\theta}_\zeta$  contains those associated to the pulse images from the secondary paths,  $\{\zeta_q(t)\}$ . Also let  $\mathbf{x}$  stand for the complete set of observations, i.e.,  $\{\mathbf{x}(t) : 0 \leq t < T_b\}$ . For the Gaussian signal model under consideration in this study, the LLF of the observations can be expressed in the form

$$\ln \Lambda(\mathbf{x}; \boldsymbol{\theta}) = -\frac{1}{2} (l_1(\mathbf{x}; \boldsymbol{\theta}) + l_2(\boldsymbol{\theta})). \quad (17)$$

The second term in (17), whose general expression can be found in [13], is not a function of the observed data and has little effect on the final estimation; we do not take it into consideration in this work.

The data-dependent term  $l_1(\mathbf{x}, \boldsymbol{\theta})$  is given by

$$l_1(\mathbf{x}; \boldsymbol{\theta}) = \sum_t \sum_u (\mathbf{x}(t) - \boldsymbol{\mu}(t))^T \mathbf{K}_x^{-1}(t, u) (\mathbf{x}(u) - \boldsymbol{\mu}(u)) \quad (18)$$

where the range of summation for both  $t$  and  $u$  is over the set  $\{nT_s : n = 0, \dots, M - 1\}$  and the quantity  $\mathbf{K}_x^{-1}(t, u)$  denotes the inverse kernel of the auto-covariance function  $\mathbf{K}_x(t, u)$  (16). The latter is defined as the solution to the inverse problem:

$$\sum_u \mathbf{K}_x(t, u) \mathbf{K}_x^{-1}(u, v) = \delta(t - v) \quad (19)$$

where  $v$  is a discrete-time variable with the same range as  $t$ . For the special form of the auto-covariance function in (16), it can be easily verified that the solution to (19) is given by:

$$\mathbf{K}_x^{-1}(t, u) = \delta(t - u) T_s (E_p \mathbf{D}(t) + \sigma_n^2 \mathbf{I}_Q)^{-1}. \quad (20)$$

Upon substitution of this expression in (17) and further manipulations, we find that

$$l_1(\mathbf{x}; \boldsymbol{\theta}) = T_s \sum_q \sum_t \frac{(x_q(t) - \sqrt{E_p} \eta(t - \tau_q))^2}{E_p g(t - T_c - \tau_q) P(t) + \sigma_n^2}. \quad (21)$$

It is of interest to examine the nature of the data processing involved in (21). According to this formula, the ML attempts to minimize the total energy in the difference signals between each one of the antenna outputs,  $x_q(t)$ , and properly scaled and time-shifted copies of the primary pulse image,  $\eta(t - \tau_q)$ . This matching process is affected by a special time-weighting which is novel in our work, and results directly from the proposed signal model in Section 2. In the high SNR regime where  $E_p \gg \sigma_n^2$ , the combined presence of the gating function and the slowly decaying APDP in the denominator of (21) has the equivalent effect of amplifying errors in the initial part of the integration period, i.e., from 0 to  $\tau_q + T_c$  where  $g(t - \tau_q - T_c) = 0$  as well as in the later part of the integral, i.e., for  $t \geq \tau_{ds} + \tau_q + T_c$ . In effect, the ML processor attempts to create a best match between  $x_q(t)$  and  $\sqrt{E_p} \eta(t - \tau_q)$  during the initial period, while ensuring that the instantaneous power in the residual signals  $x_q(t) - \sqrt{E_p} \eta(t - \tau_q)$  conforms to the available *a priori* information about the APDP. In the low SNR regime where  $E_p \ll \sigma_n^2$ , the ML processor simply measures the energy of the difference signal over the symbol duration.

## 4. ALGORITHM IMPLEMENTATION

The ML estimates of the TOA and AOA can be found by minimizing the data-dependent term (21) of the LLF, assuming that estimates of  $P(t)$  and  $\sqrt{E_p} \eta(t)$  are available. In theory, this minimization can be performed by carrying a full two-dimensional search of (21) over the set of possible values for  $\tau$  and  $\Delta\tau$ . The computational cost associated with a full search is, however, prohibitive and this approach is not feasible in practice. Next, we describe a low-cost practical alternative that consists of two steps: In the first step, we perform a coarse estimation of the TOA, based on which we then obtain a rough estimate of  $P(t)$ . In the second step, using the obtained estimates of TOA and  $P(t)$  we find the best combination of  $\tau$  and  $\Delta\tau$  that minimizes (21). These steps are discussed in detail below.

### 4.1. Step one: preliminary estimation

#### 4.1.1. Coarse TOA estimation

We start with a preliminary estimation of the TOA at each antenna. For this, we chose to use the threshold crossing (TC)-based TOA estimation method [14] due to its simplicity, although other estimation methods from the literature could be used. The TC method estimates the TOA at the  $q$ th antenna as the smallest value of time  $t$  for which the instantaneous power at the antenna output,  $x_q^2(t)$ , exceeds a given threshold  $\lambda$ , i.e.,

$$\hat{\tau}_q = \arg \min_{0 < t < T_u} \{x_q^2(t) > \lambda\} \quad (22)$$

where  $T_u$  is the search range (uncertainty region) for the TOA. In our work, the value of the threshold  $\lambda$  is adjusted experimentally to obtain the best TOA estimation performance, considering the trade-off between the early detection and miss probabilities. Using the TOA estimates  $\hat{\tau}_q$  we then obtain an LS estimate of  $\tau$  as [6, 7]

$$\hat{\tau}_{LS} = \frac{2}{Q(Q+1)} \sum_{q=0}^{Q-1} [(2Q-1) - 3q] \hat{\tau}_q \quad (23)$$

#### 4.1.2. APDP estimation

To estimate the APDP, we fit the instantaneous power at the output of the reference antenna to a single exponentially decaying model<sup>1</sup>. Let  $l_o = \lceil \hat{\tau}_{LS} / T_s \rceil$  and  $L = \lceil \tau_{ds} / T_s \rceil$  denotes the maximum channel delay spread in samples, with  $\lceil \cdot \rceil$  being the floor function. More specifically, we fit the segment of  $P_0(l) = x_0((l_o + l)T_s)^2$  from  $l = 0$  to  $L - 1$ , to the function  $\beta e^{-l\alpha}$ , with the parameters  $\alpha > 0$  and  $\beta > 0$ . We perform the curve fitting in the log domain using the LS method, i.e.,

$$\arg \min_{\alpha, \beta} \sum_{l=0}^{L-1} \mu_l |\ln P_0(l) - (\ln \beta - l\alpha)|^2. \quad (24)$$

where the weight  $\mu_l = 1$  if there is a local maximum, i.e.,  $P_0(l - 1) < P_0(l) > P_0(l + 1)$ , and  $\mu_l = 0$  otherwise. This choice of  $\mu_l$  allows us to include in the fitting only the local maxima, as they are more likely to correspond to multipath components, and to mask out the noisy low power data points [9]. Denoting as  $\hat{\beta}$  and  $\hat{\alpha}$  the solutions to (24), we obtain a coarse estimate of the APDP as

$$\hat{P}(nT_s) = \hat{\beta} e^{-\hat{\alpha}(n-l_o)}, \quad n = 0, \dots, M - 1. \quad (25)$$

We note that, the initial samples of  $\hat{P}(t)$  are not critical since they will be zeroed by the gating function  $g(t - T_c - \tau_q)$  in (21).

<sup>1</sup>This model is a simple yet effective approximation to the double-exponential decaying model suggested by the IEEE 802.15.4a task group [15].

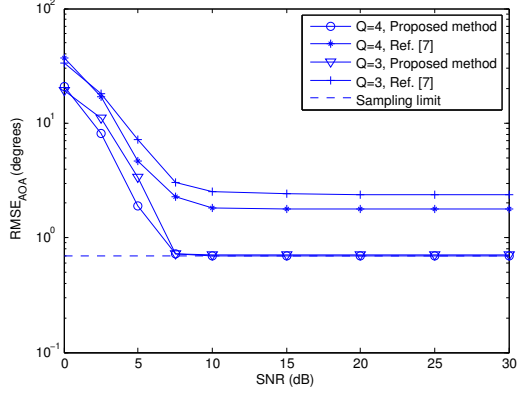


**Fig. 1.** RMSE of AOA estimates versus SNR for different number of antennas ( $F_s=16\text{GHz}$ ).

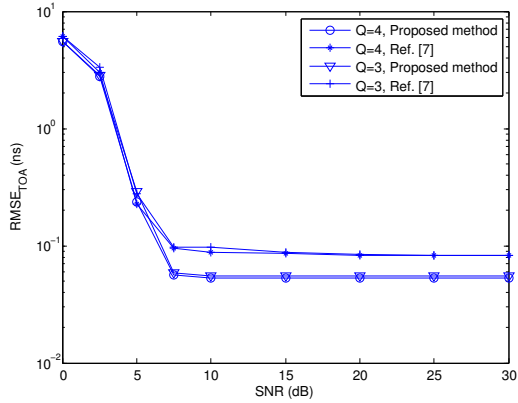


**Fig. 2.** RMSE of TOA estimates versus SNR for different number of antennas ( $F_s=16\text{GHz}$ ).

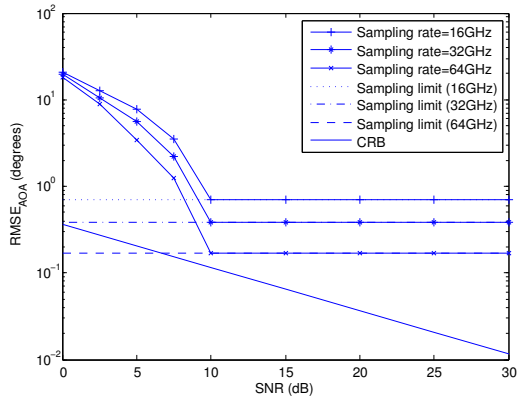


**Fig. 3.** RMSE of AOA estimates versus SNR for different sampling rates ( $Q=2$ ).

#### 4.2. Step two: joint estimation of $\tau$ and $\Delta\tau$

After obtaining  $\hat{\tau}_{LS}$  and  $\hat{P}(t)$ , we can estimate  $\tau$  and  $\Delta\tau$  by performing a two dimensional search for the combination of  $\tau$  and  $\Delta\tau$  that minimizes (21). To reduce the computational complexity, we only search for  $\tau$  in a neighbourhood around  $\hat{\tau}_{LS}$  instead of the whole uncertainty region  $T_u$ , i.e.,  $\tau \in [\hat{\tau}_{LS} - kT_c, \hat{\tau}_{LS} + kT_c]$  where  $k$  is a small integer. As for  $\Delta\tau$ , we only need to search in the

interval  $[-d/c, d/c]$  since  $|\Delta\tau| = \frac{d}{c} \cos \theta \leq d/c$ .

As can be seen from (21), to perform the search described above, we need an estimate of  $\sqrt{E_p}\eta(t)$ . To this end, for each candidate value of  $\tau$ , we estimate  $\sqrt{E_p}\eta(t)$  as the segment of  $x_0(t)$  over the interval of duration  $T_c$  starting at  $\tau$ , i.e.,

$$\sqrt{E_p}\hat{\eta}(t; \tau) = x_0(t + \tau), \quad 0 \leq t < T_c. \quad (26)$$

## 5. RESULTS AND DISCUSSIONS

In this section, the performance of the proposed joint estimator of the TOA and AOA is evaluated using computer simulations. We use a Gaussian doublet as the transmitted pulse  $w(t)$ , with duration  $T_c = 0.5\text{ns}$  and an effective bandwidth  $B = 4\text{GHz}$ . We consider the following system parameters in our experiments:  $T_b = 200\text{ns}$ ,  $T_u = 80\text{ns}$ ,  $\tau_{ds} = 120\text{ns}$  and  $N_s = 1000$ . Different values of the sampling rate  $F_s$  are employed, from 16 to 64GHz. The receiver is equipped with a ULA of  $Q \in \{2, 3, 4\}$  identical antenna elements, with inter-element spacing  $d = 50\text{cm}$ .

Channel models based on the IEEE 802.15.4a standard [15] are employed. However, to account for the presence of an antenna array at the receiver, certain modifications are made. In particular, we generate the channel response according to model CM1 (residential LOS) and then add the spacial dependency to the model according to [16, 17]. The AOA of each path follows a Laplacian distribution, with a standard deviation of  $5^\circ$  and a mean following a uniform distribution in the range  $[45^\circ, 135^\circ]$  and varying from cluster to cluster.

The root mean square error (RMSE) of both final TOA and AOA estimates are calculated. The signal-to-noise ratio (SNR) is defined as  $E_s/\sigma_n^2$ , where  $E_s$  is the energy per symbol.

Fig. 1 compares the AOA estimation performance of our proposed method to that in [7] for ULAs with  $Q = 3$  and 4 antennas and  $F_s=16\text{GHz}$ . While the AOA estimation accuracy of both methods improves with increasing the number of antennas, it can be seen that the proposed method achieves a significantly better accuracy under the same choice of parameters. At high SNR, the attainable RMSE value of the proposed method is only limited by the step size used in the ML search (represented as the sampling limit in Fig. 1). Results for TOA estimation in Fig. 2 also show a superior performance with the proposed method.

Fig. 3 compares the AOA estimation performance of the proposed method when using different sampling rates, i.e.,  $F_s=16, 32$  and  $64\text{GHz}$ . It is clearly shown that the accuracy increases as the sampling rate increases. In addition, the performance is compared to the Cramer-Rao bound as obtained in [18].

## 6. CONCLUSION

We proposed a novel joint TOA and AOA estimator for impulse radio IR-UWB systems. The proposed method consists of two steps: (1) coarse estimation of the TOA and APDP; (2) joint estimation of the TOA and AOA by maximization of a novel log likelihood function (LLF). In particular, with 2 antennas spaced 50cm apart, a SNR of 10dB and a sampling rate of 16GHz, it can provide an angular accuracy around  $0.7^\circ$  and timing accuracy of less than 0.01 ns (3cm in range). Furthermore, the accuracy improves with increasing the number of antennas.

## 7. REFERENCES

- [1] D. Dardari and R. D'Errico, "Passive ultrawide bandwidth RFID," in *Proc. IEEE Global Telecommunications Conference*, Dec. 2008, pp. 3947–3952.
- [2] N.A. Alsindi, B. Alavi, and K. Pahlavan, "Measurement and modeling of ultrawideband TOA-based ranging in indoor multipath environments," *IEEE Trans. Veh. Technol.*, vol. 58, no. 3, pp. 1046–1058, March 2009.
- [3] H. Keshavarz, "Weighted signal-subspace direction-finding of ultra-wideband sources," in *Proc. IEEE Int. Conf. on Wireless and Mobile Computing, Networking and Communications*, Aug. 2005, pp. 23–29.
- [4] V.V. Mani and R. Bose, "Direction of arrival estimation and beamforming of multiple coherent UWB signals," in *Proc. IEEE Int. Conf. on Communications*, May 2010, pp. 1–5.
- [5] E. Lagunas, M. Najar, and M. Navarro, "UWB joint TOA and DOA estimation," in *Proc. IEEE Int. Conf. on UWB*, Sep. 2009, pp. 839–843.
- [6] M. Navarro and M. Najar, "Frequency domain joint TOA and DOA estimation in IR-UWB," *IEEE Trans. Wireless Commun.*, vol. 10, no. 10, pp. 1–11, Oct. 2011.
- [7] L. Taponecco, A.A. D'Amico, and Mengali U., "Joint TOA and AOA estimation for UWB localization applications," *IEEE Trans. Wireless Commun.*, vol. 10, no. 7, pp. 2207–2217, July 2011.
- [8] Z. Sahinoglu and S Gezici, "Ranging in the IEEE 802.15.4a standard," in *Proc. IEEE Annual Wireless and Microwave Technology Conference*, Dec. 2006, pp. 1–5.
- [9] F. Shang, B. Champagne, and I. Psaromiligkos, "Joint estimation of time of arrival and channel power delay profile for pulse-based UWB systems," in *Proc. IEEE Int. Conf. on Communications*, June 2012.
- [10] H. Luecken, C. Steiner, and A. Wittneben, "ML timing estimation for generalized UWB-IR energy detection receivers," in *Proc. IEEE Int. Conf. on UWB*, Vancouver, Sep. 2009, pp. 829–833.
- [11] K. Makaratat, T.W.C. Brown, and S. Stavrou, "Estimation of time of arrival of UWB multipath clusters through a spatial correlation technique," *IET Microw. Antennas Propag.*, vol. 1, no. 3, pp. 666–673, June 2007.
- [12] G.D. Durgin and T.S. Rappaport, "Effects of multipath angular spread on the spatial cross-correlation of received voltage envelopes," in *Proc. IEEE Vehicular Technology Conference*, June 1999, pp. 996–1000.
- [13] H. L. Van Trees, *Detection, Estimation, and Modulation Theory, part III*, New York: Wiley, 1971.
- [14] D. Dardari, C.-C. Chong, and M.Z. Win, "Threshold-based time-of-arrival estimators in UWB dense multipath channels," *IEEE Trans. Commun.*, vol. 56, no. 8, pp. 1366–1378, Aug. 2008.
- [15] A.F. Molisch, K. Balakrishnan, C.C. Chong, S. Emami, A. Fort, J. Karedal, J. Kunisch, H. Schantz, U. Schuster, and K. Siwiak, "IEEE 802.15.4a channel model-final report," *IEEE 802.15 WPAN Low Rate Alternative PHY Task Group 4a (TG4a)*, Nov. 2004.
- [16] R.J.-M. Cramer, R.A. Scholtz, and M.Z. Win, "Evaluation of an ultra-wide-band propagation channel," *IEEE Trans. Antennas Propag.*, vol. 50, no. 5, pp. 561–570, May 2002.
- [17] S. Venkatesh, V. Bharadwaj, and R.M. Buehrer, "A new spatial model for impulse-based ultra-wideband channels," in *Proc. IEEE Vehicular Technology Conference*, Sep. 2005, pp. 2617–2621.
- [18] A. Mallat, J. Louveaux, and L. Vandendorpe, "UWB based positioning in multipath channels: CRBs for AOA and for hybrid TOA-AOA based methods," in *Proc. IEEE Int. Conf. on Communications*, June 2007, pp. 5775–5780.